A Novel Automated Left Ventricle Segmentation Routine

N. Liu[1], A. Trakic[1], F. Liu[1], B. Appleton[1], S. Wilson[1], R. Slaughter[2], W. Strugnell[2], S. Crozier[1]

[1]School of Information Technology and Electrical Engineering, The University of Queensland, Brisbane, QLD, Australia, [2]Cardiovascular MRI Research Centre, The Prince Charles Hospital, Brisbane, QLD, Australia

Synopsis

In this paper we present a system for the automatic segmentation of the left ventricle (LV) of the heart from breath hold MRI images with subsequent ejection fraction (EF) calculations. The ventricular luminal contours in short and long-axis slices are enhanced with morphological image processing methods and extracted using a novel Global Optimal Closed Path algorithm. In this study, contours both including and excluding LV trabeculations and papillary muscles are considered. Ventricular 3D-reconstructions are based on the use of both short-axis and long-axis contours, with the long-axis contours also being used as an internal skeleton template of the LV to correct for through plane motion. A series of volumes of the reconstructed 3D ventricle is evaluated at different times during the cycle and the EF calculated. By comparing our numerical results with those derived from manual segmentations on eight normal subjects, we conclude that the automated system performance is reliable and consistent.

Introduction

The measurement of stroke volumes and EF's from MR images is usually made using manual or semi-automated techniques. The determination of blood volume through reliable computer automated methods is an important and challenging task [1]. Our aim was therefore to design and optimize an automated system to precisely segment the LV and compute the EF. The project included two parts: contour extraction and 3D shape reconstruction from datasets acquired during breath hold on a GE 1.5T Signa Twinspeed Excite platform. These datasets consisted of cine MR image sets obtained using a steady-state free precession imaging sequence (FIESTA) with 20 cardiac phases per slice location. This resulted in 180 short-axis images (9 slice locations) and 20 long-axis images (1 slice location).

Contour Extraction

After the region of interest was cropped, image enhancement methods such as contrast adjustment, image blurring and others were used to enhance the target (lumen). Morphological operations to remove noise and refine the slices were then applied. For the long-axis slices, a moment theory method was used to register the images. The contour of the endocardium in the short-axis slice is known to be closed and close to round in nature. However, this is not always the case in some cardiac MR images, as the contour is distorted at some locations and can be difficult to determine when conventional gradient methods are used. In order to reconstruct the missing contour around the distorted contour region a variant of the Circular Shortest Path Algorithm was implemented [2, 3]. This algorithm is very successful in searching for the shortest paths of close to circular morphology in complex image terrain. If the contour is continuous and relatively strong, the path will go along it. However in regions where there is no contour or the contour is very weak, the algorithm relies on circular curves to represent the contour, and finally it evaluates the globally optimal path. After pre-processing the image, we computed the gradient of the image and used a corresponding energy functional to compose a cost distribution image. We then transferred the Cartesian to Polar coordinates and mapped the image to the grids. Finally, we applied dynamic programming to search for the global minimum cost (closed curve) path, as the starting and ending nodes are the same points. The above method is very robust for extracting contours that are roughly circular in shape, but does not work well on the long-axis slices where the contours are irregular and arbitrary in shape.

The following algorithm was used to process the long-axis images. A filter was first used to blur and smooth the image. By means of an intensity histogram, we selected the threshold for converting the image into a binary one, and then filled the holes (small black regions) inside the connected white regions. A label sorting algorithm was then applied to keep the largest (blood filled) region and remove all others. As the extracted region revealed some spurious spots attached to the boundary, we applied morphological operations (erosion and dilation) to smooth the target. The edge of the remaining white region is the derived contour of the blood-filled cavity in the long-axis slice.

The contour shown in Fig 1 (b) is the "smooth" contour, ignoring trabeculations. Fig 1(c) shows the inclusion of trabeculations. In order to accurately compute the blood volume, those small regions need to be deducted from the total area of each slice. To do this we used the smoothed contour as the mask of the original greyscale image, keeping only the region inside the mask. By adjusting the threshold, the region with the internal trabeculations could be reliably extracted. We term these contours "unsmoothed".

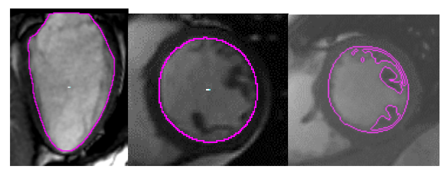

Fig 1 (a) Fig 1(b) Fig1(c)

Fig 1 Short-axis and long-axis Contours

Shape Adjustment and 3D Visualization

The short-axis slice is perpendicular to the long axis. If we project the short-axis slices onto the long axis slice, each short-axis slice can be viewed as a line (Fig 2 (a) (b)). For a number of reasons, the contour in the short-axis slice does not accurately match the corresponding line in the long-axis. We adjusted the size of the short-axis contour to match its corresponding line in long axis by computing the area of a circle with that line as its diameter. The result is shown in Fig 2(c). Fig 2 (d) illustrates a 3D reconstructed ventricle.

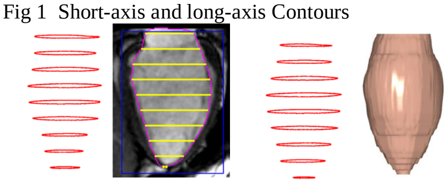

Fig 2(a) Fig 2(b) Fig 2(c) Fig 2(d)

Fig 2 Contours adjustment and 3D LV

EF Comparison

Figure 3 shows a Bland-Altman plot [4] of 8 paired observations. The comparison of EF's between manual and automated results shows very good agreement. The bias and precision [mean of the difference between expert and automated EF calculations ± 2 standard deviations (SD's)] was -0.016 ± 0.028 in the smoothed case and –0.007± 0.012 in the unsmoothed case. This result would be improved if more slices were acquired. EF-smooth is the EF computed from the smooth short-axis contours. Since the results of the smoothed and unsmoothed EF's are very similar, there is presumably little effect on EF from LV trabeculations.

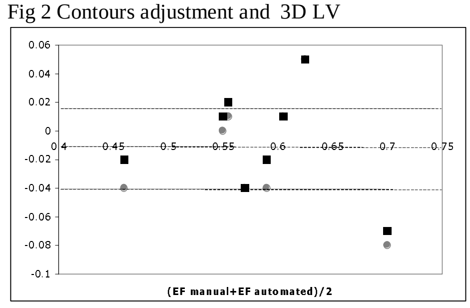

Fig 3 Bland Altman plot of expert (manual) EF measure compared to smoothed (circle) and unsmoothed (square) automated EF measure. Smoothed mean and ±2SD's (dashed) are shown.

Conclusion

In this paper, we have introduced an automated EF evaluation system, including image pre-processing, contour detection, shape adjustment and 3D reconstruction. MR images from eight normal subjects are employed to test the system. The EF values derived from the automated system and those values derived manually are in good agreement. This technique should improve the efficiency and reproducibility of EF extraction.

References

[1] van der Geest RJ, Buller VG, Jansen E, Lamb HJ, Baur LH, van der Wall EE, de Roos A, Reiber JH., Comparison between manual and semiautomated analysis of left ventricular volume parameters from short-axis MR images. *J Comput Assist Tomogr*. 1997 Sep-Oct;21(5):756-65

[2] B. Appleton and C. Sun. Circular shortest paths by branch and bound, *Pattern Recognition*, 36(11):2513- 2520, Nov 2003.

[3] C. Sun and S. Pallottino. Circular shortest path in images. *Pattern Recognition*,36(3):709-719, Mar 2003

[4] JM Bland and DG Altman. Statistical Methods for Assessing Agreement Between Two Methods of Clinical Measurement, *The Lancet*, February 8, 1986, 307-310.